

## STUDY OF Zn–Co ALLOY COATINGS MODIFIED BY NANO- TiO<sub>2</sub> PARTICLES INCORPORATION

M. DIAFI<sup>a\*</sup>, A. AIDI<sup>b</sup>, B. BENHAOUA<sup>c,d</sup>

<sup>a</sup>*Physic Laboratory of Thin Films and Applications (LPCMA), University of Biskra, Algeria*

<sup>b</sup>*Department of Chemical Industry, University of Biskra, Algeria*

<sup>c</sup>*Unit of Renewable Energy Development in Arid Zones (UDERZA), Univ. El-Oued, El Oued 39000, Algeria*

<sup>d</sup>*Lab. VTRS, Faculty of Technology, Univ. El-Oued, El oued 39000, Algeria*

The purpose of this paper is to investigate the effect of TiO<sub>2</sub> nanoparticles contents on structural properties, microhardness and corrosion resistance of Zn-Co alloy coating and Zn-Co-TiO<sub>2</sub> composite coatings is electrodeposited on steel substrate in the acid sulfate bath, The smaller grain size of the composite coatings is observed in the presence of TiO<sub>2</sub> and it is confirmed by the images of scanning electron microscopy (SEM) and X-ray diffraction (XRD) techniques. The corrosion performance of coating in the 3 % NaCl as a corrosive solution is investigated by potentiodynamic polarization and electrochemical impedance spectroscopy EIS methods. It is found that the incorporation of nanoparticules in Zn–Co alloy coating have better corrosion resistance and the values of  $R_{ct}$  and  $Z_w$  increase, while the values of  $C_{dl}$  decrease with the increasing of nanoparticules.

(Received January 29, 2020; Accepted July 4, 2020)

*Keywords:* Alloy, TiO<sub>2</sub> nanoparticles, Zinc, Microhardness, Electrodeposition, Corrosion resistance

### 1. Introduction

Electroplated binary Zn-Malloys, where metals are an Fe group such as Fe, Co, Sn, Ni, Mn and Cr [1-3], exhibit improved properties compared to pure Zn is nowadays of great importance not only for corrosion protection of metallic substrates but also used in a variety of industrial applications, one of the first applications such as catalysts, electrodes for batteries, magnetic uses [4-6] and printing plates the most common examples are being Zn–Fe [7–8], Zn–Co [9-12] and Zn–Ni [13–16], It is believed that the composition and corrosion resistance of composite coatings are influenced by several interrelated parameters, such as chemical composition of the electrolyte, the concentration of metal ions solution temperature and pH, agitation, type of applied current and current density [17].

Electrodeposited composites are obtained by adding insoluble solid particles to an electrolytic bath [18]. These insoluble particles can be oxides such as (Al<sub>2</sub>O<sub>3</sub>, TiO<sub>2</sub>, ZrO<sub>2</sub>, SiO<sub>2</sub>, SiC ).They are used as a second phase because they possess good chemical stability, provide better mechanical properties, and good wear resistance and corrosion resistance at elevated temperature [13,18]. Zn–Co composite coatings for example ZnCo–Al<sub>2</sub>O<sub>3</sub> and ZnCo–SiC [19], TiO<sub>2</sub> have been used to improve different metallic and organic coatings. TiO<sub>2</sub> with a metallic coating, significantly contributes to wear and corrosion resistance, better hardness [20-21]. In their works, indicated (who) that the porous nanocomposite coatings exhibit higher corrosion resistance when compared to Zn–Co coatings and it is strongly affected by the TiO<sub>2</sub> structure and concentration, The composite coatings has been characterized, morphological (SEM), (XRD), and electrochemical properties of the composite coatings had been studied by potentiodynamic polarization and electrochemical impedance spectroscopy in a solution of 3 % NaCl.

---

\*Corresponding author: m.diafi@univ-biskra.dz

## 2. Experimental details

### 2.1. Coating preparation

Nanocomposite coatings Zn–Co, with different concentrations of nanoparticles of TiO<sub>2</sub>, have been prepared on mild steel substrates form plates (25mm x 5mm x 2mm) which were used as cathode electrode, by electrodeposition technique. The zinc plates were used as anodic electrodes. The distance between the anode and the cathode is maintained at 2 cm to ensure deposit uniformity. Before deposition, the substrates were polished mechanically, degreased in alkaline solution, treated in HCl (10 %) solution, cleaned in acetone and then rinsed with distilled water. The process was carried in sulphate bath at current density of 30 mA cm<sup>-2</sup> and temperature of 30°C during 30 minutes. The chemical composition of the basic electrolyte of Zn–Co alloys deposition is given in Table 1. Electrodeposits Zn–Co is obtained by varying the concentration of TiO<sub>2</sub> in the bath (5, 10, 20 g·l<sup>-1</sup>).

Table 1. Solution composition and conditions for alloy electroplating [9, 26].

Electrolyte I	Concentration (g·l <sup>-1</sup> )	Plating parameters
ZnSO <sub>4</sub> ·7H <sub>2</sub> O	57.5	30°C and pH=3,5 constant current densities at 30 mA cm <sup>-2</sup> for 60s
CoSO <sub>4</sub>	52.5	
H <sub>3</sub> BO <sub>3</sub>	9.3	
Na <sub>2</sub> SO <sub>4</sub>	56.8	
Na <sub>3</sub> C <sub>6</sub> H <sub>5</sub> O <sub>7</sub>	56.8	

### 2.2. Coating characterization

The phase structure of the coatings is determined using X-ray diffraction with a D8 Advance-Brucker using a Cu K $\alpha$  radiation ( $\lambda = 1.5406 \text{ \AA}$ ) and  $2\theta = 0.02^\circ$  as a step.

Scherrer's formula is used for the determination of the coatings crystallite sizes from the X-ray peak broadening of the (101) diffraction peak at [9.27]:

$$D = \frac{0.9\lambda}{\beta \cos\theta} \quad (1)$$

where D is the grain size,  $\lambda$  is the X-ray wavelength,  $\beta$  is the corrected peak full width at half-maximum intensity (FWHM), and  $\theta$  is Bragg angle position of the considered peak.

The deposits surface morphology was studied by scanning electron microscopy (A JEOL model JSM6390LV).

Microhardness of coatings is was measured using a load of 100 g with a holding time of 15s by using a Vickers hardness tester, and the average of ten hardness measurements was quoted as the hardness value.

The corrosion behavior and the protection performance of Zn-Co alloy and Zn-Co- TiO<sub>2</sub> composite coatings were studied by using electrochemical impedance spectroscopy (EIS) and electrochemical Tafel extrapolation (TE) in 3,5 % wt NaCl solution. The tests were performed using a potentiostatgalvanostat (a Volta Lab 40 model). A coated sample was served as a working electrode, the counter electrode was platinum with a surface of 1 cm<sup>2</sup> and the Hg/HgO/ 1 M KOH is used as a reference electrode. The impedance data were obtained at open-circuit potential and the measurements were carried out over a frequency range of 100 kHz-10 MHz using the amplitude of sinusoidal voltage (10mV). Potentiodynamic polarization with a scan rate of 50mV/s was applied in order to study the anodic dissolution of the coatings. The corrosion current density (I<sub>corr</sub>) and corrosion potential (E<sub>corr</sub>) were determined using TE.

### 3. Results and discussion

#### 3.1. Phase structure

Fig. 1 shows XRD patterns for four Zn-Co alloy coating and Zn-Co-TiO<sub>2</sub> composite coatings. The metallic phases are well crystalline and can be ascribed to the Zn hexagonal structure in Fig 1(a). Only the diffraction lines of zinc-rich ( $\eta$ -phase) (JCP: 4-0831 [19]) and cubic Co<sub>5</sub>Zn<sub>21</sub> phase ( $\gamma$ -phase) (JCPDS N: 22-0521). The presence of TiO<sub>2</sub> diffraction lines in the X-ray spectra of the deposits Fig. (1 .d) confirmed also the formation of the Zn–Co–TiO<sub>2</sub> composite layers. The analysis of diffractograms shows that the composition of the plating bath has a strong influence on the crystal orientation in the deposit. Thus, the diffraction maximum (101) of Zn-Co in the composite layers decreases, These results are in accordance with those stated in the literature, that the particles embedded in the coatings can affect the preferred orientation of the metallic matrix as a consequence of changes on the metal deposition mechanism [21].

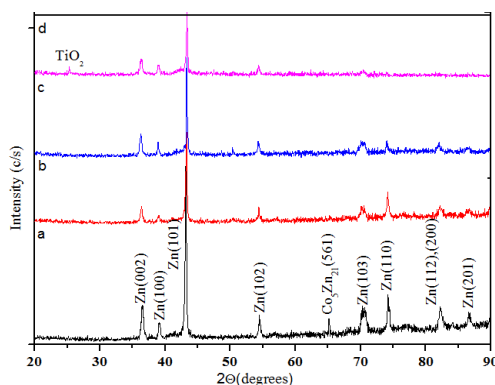


Fig. 1. XRD spectra of (a) Zn-Co alloy coatings and (b) Zn-Co-TiO<sub>2</sub> (5 g/l TiO<sub>2</sub>), (c) Zn-Co-TiO<sub>2</sub> (10 g/l TiO<sub>2</sub>), (d) Zn-Co-TiO<sub>2</sub> (20 g/l TiO<sub>2</sub>) Composite coatings.

Crystallite sizes were determined using the Scherer formula. For all coatings, the profile of (101) peak exhibits Lorentzian line shape, like shown as it is showed in Table 2.

Table 2. Values of the crystallite size obtained from the strongest diffraction line of the metallic phases.

Electrolyte	hkl	2θ(°)	Crystal size (nm)
Zn-Co (0 g/l TiO <sub>2</sub> )	(101)	43.15	55.99
Zn-Co-TiO <sub>2</sub> (5 g/l TiO <sub>2</sub> )	(101)	43.18	43.08
Zn-Co-TiO <sub>2</sub> (10 g/l TiO <sub>2</sub> )	(101)	43.28	39.05
Zn-Co-TiO <sub>2</sub> (20 g/l TiO <sub>2</sub> )	(101)	43.39	30.77

The grain sizes significantly decrease from 55.99nm to 43.08 nm with increasing TiO<sub>2</sub> nanoparticles concentration from zero to 5g/l in the electrolyte, and slowly decreases for a concentration more than 10 g/l, 20 g/l (Table 2), indicates that the composite coatings have smaller grain size than alloy coatings. Therefore, incorporation of TiO<sub>2</sub> nanoparticles in the coating refined the crystals. It is worth noting that all coatings grain sizes are in the nanometer scale, confirming the nanocrystalline structure of Zn-Co and Zn-Co-TiO<sub>2</sub> composite coatings. This finer structure may be at the origin of the decrease in the whole peaks intensity of the coated steel substrates and may be at the origin of the higher hardness of this deposit as mentioned previously [22,23].

### 3.2. Surface morphology

The morphology of these coatings plated in different compositions and for two magnifications 20 and 30  $\mu\text{m}$  is presented in fig. 2(a-d). It is clearly shown that in general, the surface of the Zn-Co alloy coating (fig. 2 a) is uniform, homogenous and consists of irregular crystals particles with a clear grey color [9], the grain size of the Zn-Co-TiO<sub>2</sub> composite coating (fig. 2 a, b, and d) sample is smaller and more uniform crystals when compared with the Zn-Co coating. As it is seen in fig. 2 b. The incorporation of TiO<sub>2</sub> nanoparticles, with feeble amount, in the Zn-Co coating retards the crystal growth and leads to a smaller grain size [24]. Whereas for Zn-Co-TiO<sub>2</sub>(10 g / l TiO<sub>2</sub>), the grains become greater having rocky-like shape as seen in fig. 3c (not the same magnification 30  $\mu\text{m}$ ) then they become separated rocky-like shape (see fig. 3d) for the least concentration of TiO<sub>2</sub> (10g/l).

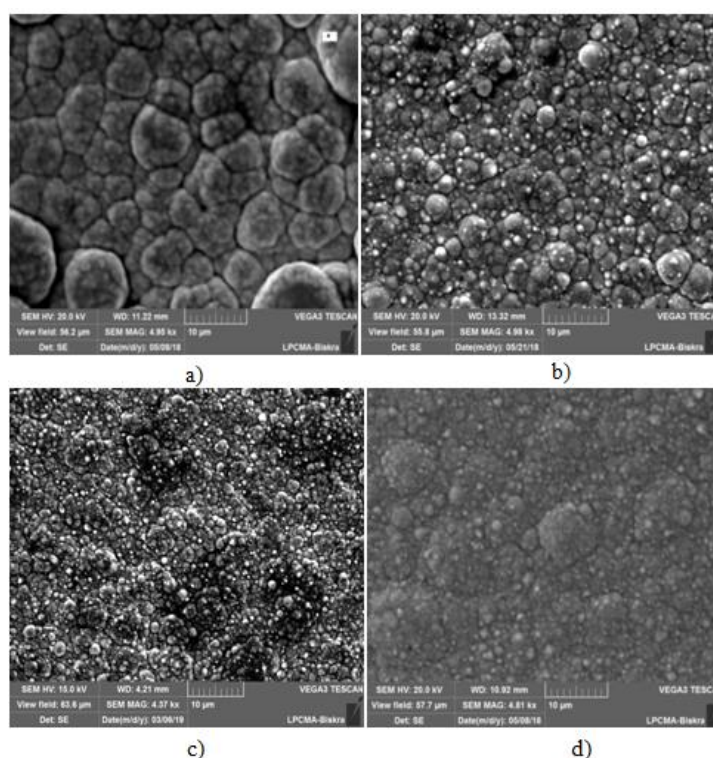


Fig. 2. Surface morphology of (a) Zn-Co alloy coatings and (b) Zn-Co-TiO<sub>2</sub> (5 g / l TiO<sub>2</sub>), (c) Zn-Co-TiO<sub>2</sub> (10 g / l TiO<sub>2</sub>), (d) Zn-Co-TiO<sub>2</sub> (20 g / l TiO<sub>2</sub>) Composite coatings.

### 3.3. EDX analysis of the Zn-Co-TiO<sub>2</sub> composite coating

For further analysis of alloy coatings nanoparticles EDAX analysis is used, Fig. 3 (a-c) for Zn-Co-TiO<sub>2</sub> (5, 10, and 20 g / l TiO<sub>2</sub>) confirms the presence of TiO<sub>2</sub> in those alloys. This analysis showed also a doublet signal peak for TiO<sub>2</sub> at 0.5 and approximately 5.5 keV.

Chemical compositions of Zn-Co-TiO<sub>2</sub> composite coatings depend on the concentration of TiO<sub>2</sub>, as shown in Fig 3. Also EDAX analysis shows that the Co content increases from 22% to 27% with increasing TiO<sub>2</sub> concentration in bath. The study of the impact of the TiO<sub>2</sub> nanoparticles in nucleation and growth of the Zn-Co films is in progress [22,25].

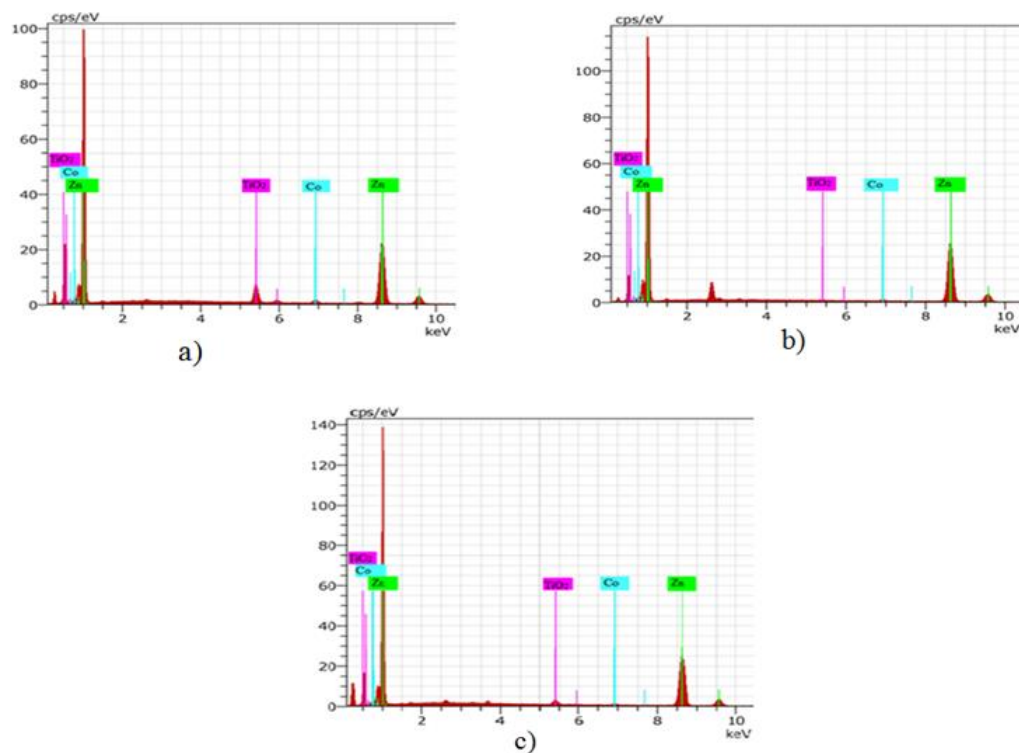


Fig. 3.EDAX of a) Zn-Co-TiO<sub>2</sub> (5 g /l TiO<sub>2</sub>), (b) Zn-Co-TiO<sub>2</sub> (10 g /L TiO<sub>2</sub>), (c) Zn-Co-TiO<sub>2</sub> (20 g /l TiO<sub>2</sub>) Composite coatings.

### 3.4. Micro hardness measurements

The microhardness results of Zn-Co alloy and Zn-Co-TiO<sub>2</sub> composite coatings electroplated at different agitation speeds are summarized in Table 2. The results indicated that Zn-Co-TiO<sub>2</sub> composite coatings showed higher microhardness compared to Zn-Co alloy coatings. The variation of microhardness results can be attributed to the incorporation of TiO<sub>2</sub> nanoparticles. The upper hardness of the coating is because of the deposit formation with fine-grained structure. As explanation to this hardness is that during its measurements, the easy movement of dislocations has been obstructed by the dispersed particles in the fine-grained matrix which is shown in the case of composite coated samples. The hardness of nanocomposite coating depends directly on the TiO<sub>2</sub> content of nanocomposite coating [20,22,25].

Table 3. Values of micro-hardness Vickers hardness (HV) registered different electro deposition.

Coating	hardness
Zn-Co	177.8
Zn-Co-TiO <sub>2</sub> ( 5 g /l)	212
Zn-Co-TiO <sub>2</sub> ( 10 g /l)	250
Zn-Co-TiO <sub>2</sub> ( 20 g /l)	283

### 3.5. Potentiodynamic polarization studies

Tafel tests have been performed on Zn-Co alloy and Zn-Co-TiO<sub>2</sub> composite coatings in 3.5 % NaCl solution. Tafel polarization readings have been shown in Fig 4. The corresponding electrochemical parameters extracted from Tafel plots are summarized in Table 3. Results indicated that the corrosion potentials of Zn-Co-TiO<sub>2</sub> composite coatings shift to the positive direction and corrosion current density decreased significantly compared to Zn-Co alloy coatings. The Zn-Co-TiO<sub>2</sub> nanocomposite coatings have lower chemical activity than the Zn-Co

alloy coating and hence possess better chemical stability in the external environment. The better electrochemical performance of the Zn-Co-TiO<sub>2</sub>nanocomposite coatings may be attributed to the reduction in the defect size of the nanocomposite coatings by the incorporation of nanoparticles, which is helpful to diminish the surface in contact with the corrosive environment also help to prevent the corrosive pits from growing up, and the incorporation of nano-particulates contributes to accelerate the passivation process of the metal matrix as well. Subsequently, the corrosion resistance of the nanocomposite coatings was improved [20,22-25].

Table 4. Electrochemical parameters of the coatings derived from Tafel plots.

Coating	E <sub>corr</sub>	i <sub>corr</sub>	B <sub>a</sub>	B <sub>c</sub>	R <sub>p</sub>
Zn-Co	-430,4	2,9868	59,1	-36,1	4,25
Zn-Co- TiO <sub>2</sub> (5 g /l)	-401,7	1,3819	80,9	-87,3	8,61
Zn-Co- TiO <sub>2</sub> (10 g /l)	-389,6	0,9141	51,3	-48,4	11,64
Zn-Co- TiO <sub>2</sub> (20 g /l)	-349,1	40,3	-79	15,86	

### 3.6. Electrochemical impedance spectroscopy

EIS is a useful technique for ranking coatings [1, 9]. Fig. 5 shows the EIS Nyquist plots of the three alloys in 3,5% NaCl solution, where  $Z'(\omega)$  and  $Z''(\omega)$  are the real and imaginary parts of the measured impedance, respectively, and  $\omega$  is the angular frequency. The significantly higher impedance and larger diameter of the (incomplete) semicircle in the spectra of the ternary alloy reflect its high corrosion resistance, which can be related to a change in the film (coating) capacitance  $C_f$ , and not only control by the charge transfer resistance  $R_{ct}$ . The capacitive impedance at high frequencies is well related to the thickness and to the dielectric constant of the coating. From the data obtained in Table 4, one can conclude that the values of  $R_{ct}$  and  $Z_w$  increase, while the values of  $C_{dl}$  decrease with the increasing of TiO<sub>2</sub> nano-particles content, and this behavior is in good agreement with that obtained for the Tafel plot measurements. The spectra presented shows at least two time constants. The first time constant, recorded at higher frequency, is displayed as a depressed incomplete semicircle. The electrical-equivalent-circuit (EEC) parameters, describing the process included in this time constant are  $R_{ct}$  and  $C_{dl}$  [13]. The second time constant, depicted at lower frequencies, corresponds to a straight line Figs 6. This linear dependence between the imaginary and real part of the capacitance is related to the diffusion process of the soluble species, while is called Warburg impedance ( $Z_w$ ) Therefore, EEC parameters describing the process included in the second time constant clearly indicates the diffusion control of the soluble species. From the electrode surface to the bulk of solution [20]. Zn-Co-TiO<sub>2</sub> provides better protection against corrosion on the steel substrate [13]

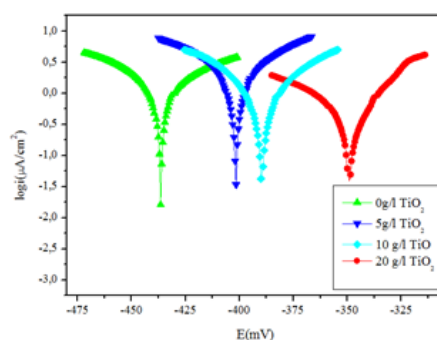


Fig. 4. Polarizing curves obtained for the alloy coatings in a 3.5 % NaCl solution at different concentrations of TiO<sub>2</sub> nanoparticles.

Table 5. Simulation parameters obtained at the abandonment potential.

Coatings	$R_e$ [ $\Omega.cm^2$ ]	$R_{ct}$ [ $\Omega.cm^2$ ]	$C_{dl}$ [F. $cm^2$ ]	$Z_w$ [ $\Omega.cm^2$ ]
Zn-Co	6.579	0.934	0.159	1.253
Zn-Co- TiO <sub>2</sub> (5 g /l)	6.058	0.991	0.123	3.752
Zn-Co- TiO <sub>2</sub> (10 g /l)	7.017	1.275	0.027	4.128
Zn-Co- TiO <sub>2</sub> (20 g /l)	8.417	2.322	0.019	5.546

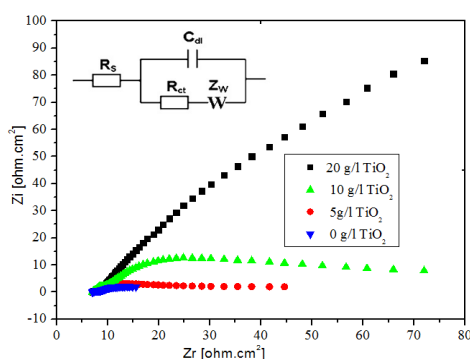


Fig. 5. Impedance diagrams for Zn-Co alloy and Zn-Co-TiO<sub>2</sub> composite coatings samples in 3% NaCl solution.

#### 4. Conclusions

In this study, the effect of TiO<sub>2</sub> nanoparticles contents, in bath, on structural properties, microhardness and corrosion resistance of Zn-Co alloy coating have been investigated. The coatings have been deposited on mild steel substrates by electrodeposition from a sulfate bath. Results from this investigation can be drawn by the following points:

XRD and SEM results indicate that Zn-Co alloy coating Zn-Co-TiO<sub>2</sub> composite coating form a mixture of two phases, zinc and cubic Co<sub>5</sub>Zn<sub>21</sub> phases, with smaller crystallite size,

The deposited coating with 20 g/l TiO<sub>2</sub> showed the maximum value of hardness 283HV, because of the increase of TiO<sub>2</sub> nano-particles concentration in the plating bath.

Polarization resistances of Zn-Co composite coating increased with the increasing of the TiO<sub>2</sub> nano-particles content.

The data obtained from electrochemical impedance spectroscopy (EIS) assumes that, the charge transfer resistance ( $R_{ct}$ ) is higher and the capacity of the double layer ( $C_{dl}$ ) value is lower for Zn-Co-TiO<sub>2</sub> composite coating containing 20 g /l TiO<sub>2</sub> alloy compared with those of Zn-Co matrix. This behavior is in good agreement with that obtained from Tafel plot measurements.

#### Acknowledgments

I would like to thank "Responsible of Physics Laboratory of Thin Films and Applications (LPCMA)" for their assistance in the preparation of this work.

#### References

- [1] M. Diafi, N. Belhamra, B. T. Hachemi, B. Gasmi, S. Benramache, Acta Metallurgica Slovaca **21**, 226 (2015).



- [2] A. Conde, M. A. Arenas, J. J. de Damborenea, *Corrosion Science* **53**, 1489 (2011).
- [3] S. Ghaziof, W. Gao, *Applied Surface Science* **311**, 635 (2014).
- [4] S. Fashu, C. D. Gu, J. L. Zhang, H. Zheng, X. L. Wang, J. P. Tu, *Journal of Materials Engineering and Performance* **24**, 434 (2015).
- [5] G. D. Wilcox, D. R. Gabe, *Corrosion Science* **35**, 1251 (1993).
- [6] N. Boshkov, K. Petrov, S. Vitkova, and G. Raichevsky, *Surface & Coatings Technology* **194**, 276–282 (2005).
- [7] A. B. Velichenko, J. Portillo, X. Alcobe, M. Sarret, C. Muller, *Electrochimica Acta* **46**, 407–414 (2000).
- [8] G. D. Wilcox, D. R. Gabe, *Corrosion Science* **35**, 1251–1258 (1993).
- [9] M. Diafi; L. Tahraoui; K. Digheche; F. Khamouli, *Acta Metallurgica Slovaca* **24**, 241–250 (2018).
- [10] K. Higashi, H. Fukushima, T. Urokawa, T. Adanya, K. Matsudo, *Journal of Electrochemical Society* **128**, 2081 (1981).
- [11] E. Gomez, E. Valles, *Journal of Electroanalytical Chemistry* **421**, 157 (1997).
- [12] R. Fratesi, G. Roventi, G. Giuliani, C. R. Tomachuk, *Journal of Applied Electrochemistry* **27**, 1088 (1997).
- [13] M. Diafi, S. Benramache, E. G. Temam, M. L. Adaika, B. Gasmi, *Acta Metallurgica Slovaca* **22**, 171 (2016).
- [14] L. Felloni, R. Fratesi, E. Quadrini, G. Roventi, *Journal of Applied Electrochemistry* **22**, 657 (1992).
- [15] G. Barcelo, J. Garci, M. Sarret, C. Muller, J. Pregonas, *Journal of Applied Electrochemistry* **24**, 1249 (1994).
- [16] M. Mouanga, L. Ricq, P. Berçot, *Surface and Coatings Technology* **202**, 1645 (2008).
- [17] S. Ghaziof, P. A. Kilmartin, W. Gao, *Journal of Electroanalytical Chemistry* **755**, 63 (2015).
- [18] S. Pouladi, M. H. Shariat, M. E. Bahrololoom, *Surface and Coatings Technology* **213**, 33 (2012).
- [19] P. C. Tulio, I. A. Carlos, *J. Appl. Electrochem.* **39**, 1305 (2009).
- [20] N. Belhamra, A. R. Boulebtina, K. Belassadi, A. Chala, M. Diafi, *Diffusion Foundations* **18**, 19 (2018).
- [21] A. Vlasi, S. Varsara, A. Pop, C. Bulea, L. M. Muresan, *J. Appl. Electrochem.* **40**, 1519 (2010).
- [22] A. Gomes, I. Almeida, T. Frade, A. C. Tavares, *Materials Science Forum* **636**, 1079 (2010).
- [23] B. M. Praveen, T. V. Venkatesha, *Applied Surface Science* **254**, 2418 (2008).
- [24] B. M. Praveen, T. V. Venkatesha, *International Journal of Electrochemistry* **2011**, 1 (2011).
- [25] D. Blejan, D. Bogdana, M. Pop, A. V. Pop, L. M. Muresan, *optoelectronics and advanced materials* **5**, 25 (2011).
- [26] M. Diafi, K. Degheche, H. Ben Temam, *Journal of Fundamental and Applied Sciences* **9**, 89 (2017).
- [27] M. Diafi, M. Omari, *Boletín de la Sociedad Española de Cerámica y Vidrio* **51**, 337 (2012).